Available online at www.sciencedirect.com

ScienceDirect

Procedia Structural Integrity 33 (2021) 734–747

Structural Integrity Procedia

www.elsevier.com/locate/procedia

IGF26 - 26th International Conference on Fracture and Structural Integrity

Finite Element Analysis of OT Bridge fixed prosthesis system

Dario Milone[a]*, Fabiana Nicita[a], Gabriele Cervino[b], Dario Santonocito[a], Giacomo Risitano[a]

[a]*University of Messina, Department of Engineering, Contrada di Dio (S. Agata), 98166 Messina, Italy*
[b]*University of Messina, Biomorf Department, School of Dentistry, Policlinico G. Martino, Via Consolare Valeria, 98124 Messina, Italy*

Abstract

The aim of this paper has been to define the behaviour of an OT Bridge fixed prosthesis system (Rhein83®). Through the use of finite element analysis, the typical load conditions of the chewing dynamics were studied, in order to highlight possible errors of inadequate use of the implant itself. These techniques highlight how knowledge of the stresses produced on the implant prosthesis becomes necessary and indispensable. The innovation in this retention system lies in the use of Seeger rings in acetal resin. The Seeger ring constitutes a revolution in the concept of anchoring the prosthesis; having a retentive function, it prevents the screws from unscrewing by taking most of the retentive load.

Keywords: fixed prosthesis; OT-Bridge; edentulism; FEM.

1. Introduction

The evolution of the characteristics of the materials, the engineering approaches and the clinical protocols have optimized the use of implant-prosthetic rehabilitations, in order to increase the comfort and chewing performance of edentulous patients. The surgical positioning of the implants based on prosthetic planning determines an optimal achievement of aesthetics and functionality (Kiatkroekkrai et al., 2020).

* Corresponding author. Tel.: +39 3396742694.
E-mail address: dmilone@unime.it

10.1016/j.prostr.2021.10.081

Computer-guided surgery has made an excellent contribution to planning the placement of prosthetically guided implants through an accurate pre-surgical evaluation of bone availability and a pre-visualization of the final prosthesis (Tallarico et al., 2019, 2016) In the recent years, dental research has focused heavily on the problem of prosthetic failure. The most common complications are related to the lack of prosthetic space or bad prosthetic design, phonetic and aesthetic problems and the maintenance of oral hygiene (Zitzmann et al., 2008). High tension concentrations at bone-implant interface may activate the biological bone resorption causing peri-implant bone loss followed by implant failure (Romeo et al., 2002; Roos-Jansåker et al., 2006).

The knowledge of the distribution of tensions and deformations in maxillary bones and in implants is of fundamental importance for the evaluation of osseointegration and adequate stability of the implant itself. A significant contribution to the study of prosthesis failures is given by finite element analysis (FEA) which simulates the real behaviour of the components under predefined load conditions. The inclination of the dental implants is also an important factor in the long-term survival of implant-supported prostheses. Numerical simulations show that an inclined position of the implant, with respect to its load axis, generates rotation effects on the device itself and torsional effects in the bone (Cicciù et al., 2019, 2018). This causes an uneven distribution of loads in the maxillary bones with large areas where tensions exceed the bone resorption threshold (Cicciù et al., 2018). The positioning of tilted implants, due to reabsorbed alveolar ridges with the risk of damaging the surrounding anatomical structures, has encouraged the use of customized or angled abutments and milled or cast bars to improve the emergence profile of the prosthesis (Chatterjee et al., 2015; Moeller et al., 2011; Sannino and Barlattani, 2016). However, commercially available angled abutments correct only moderate disparallelism (from 15° to 35°) and can cause more stress on implants, adjacent bone and prosthetic components (Cavallaro and Greenstein, 2011; Kao et al., 2008; Lin et al., 2008). A recent systematic review has reported a greater risk of implant failure (due to the eccentric load distributed on the implant) and of loosening and fractures of the abutment screw when using angled abutments (Omori et al., 2020). Other studies have shown that the internal connection and antirotational design cause a lower risk of loosening the abutment screw (Huang and Wang, 2019). The height of the abutment can influence the bone margin during healing (Chen et al., 2019) and that repeated detachment and connection of the abutment increases the marginal bone loss (Tallarico et al., 2018).

The idea of the OT Bridge fixed prosthetic system (Rhein83, Bologna, Italy) was born from the need to overcome the disadvantages in the use of angled abutments, greatly simplifying the prosthetic procedures (Tallarico et al., 2020). The choice of reliable and predictable implant-prosthetic systems is indispensable in dental clinical practice, as well as in improving the quality of life from both an aesthetic and functional point of view (Scrascia et al., 2020). This system is based on the use of the low profile OT Equator attachment, already on the market to provide retention for implant retained overdentures (Cervino et al., 2019; Gandhi et al., 2019; Scrascia et al., 2018). The morphology of this attachment has greater fracture resistance and allows a better distribution of the load to the surrounding tissues, improving peri-implant bone levels (Cervino et al., 2019).

The innovation of the OT Bridge system consists in the use of an extragrade titanium abutment and a Seeger system that guarantees the connection stability between abutment and OT Equator and passivation in the presence of serious disparallelisms. This represents a revolution in the anchoring concept as the Seeger, positioning itself inside the extragrade abutment, guarantees excellent stability in the prosthetic structure regardless of the presence of the connection screw.

The aim of this paper is to define the behaviour of the OT Bridge prosthetic system through FEM analysis by assessing the stresses generated on the prosthesis and on the bone-implant system and stability. Loading conditions typical of chewing dynamics are applied in order to highlight possible errors of inadequate use of the prosthesis studied.

2. Materials and Method

2.1. OT Bridge

The fixed OT Bridge prosthesis has numerous advantages that make it a simple and versatile rehabilitation treatment as well as functional and safe.

The low-profile attachment (OT Equator) derives from the ball attachment for overdenture, but the neck and head of the sphere are eliminated and the equatorial part is maintained. It also has an internal thread in the center of the attachment for the connection screw without transverse screws as in the angled abutments. The OT Equator is a much more resistant structure than a multi-unit abutment because it has larger diameters and its locking screw is 30% larger ensuring greater resistance. Being a one-piece attachment, it does not need a through screw thus reducing the risk of fracture. The abutment has an internal design with extragrade system and it must be positioned with the extragrade bevel in the direction of the undercut created by the inclination of the implant. An external flat surface identifies the position of the extragrade bevel. The abutment has a dedicated groove inside which an open ring in acetal resin (Seeger) is inserted. The Seeger widens to overcome the head of the Equator and returns to its original form when it reaches the base of the attachment. Moreover, it determines a monoblock connection between OT Equator and the abutment ensuring absolute passivity. In the abutment there is also an anti-rotation system thanks to which the Seeger will only have a certain position.

The OT Bridge system is related to the concept of "one abutment at one-time". Respect for biological width is fundamental for the prevention of peri-implant bone resorption (Santonocito et al., 2021) and thus for the long-term survival of the osseointegrated implants. The procedure involves screwing the Equator attachments over the implants during the first or second surgical period without removing them. This approach will guarantee stability to the desmosomial and connective attachment of the peri-implant junction which will not be violated until the delivery of the prosthesis. Furthermore, the absence of a locking screw reduces the contamination and bacterial proliferation inside the implant.

Since the OT Equator is a low-profile attachment, a first advantage is related to the size. Connections with a height of 0.5 mm and 2 mm are available respectively for systems with internal and external connection. Therefore, the shape and size of these attachments allow to obtain an excellent result even in aesthetic areas.

Another important aspect is related to the Seeger's retentive force. The tightness of the extragrade abutment on the attachment is not linked so much to the presence of the connecting screw but to the mechanical retention given by the Seeger. The clinician will be able to use the abutments in "blind mode" without any connection screw, entrusting the connection only to the Seeger. Thus, it is possible to realize a fixed full arch prosthesis by avoiding anaesthetic holes for the connection screws.

2.2. Reverse engineering

Fem studies of the following elaborate were carried out based on a resin jaw model (Fig. 1a), on which the prostheses were implanted. The first phase was characterized by the acquisition of the exact dimensions of the jaw and the positions of the implants on it. For this reason, the authors used a scanner (Fig. 1c) to acquire the size of the jaw with an GOM ATOS compact (resolution 8-12 Mpixel).

This process was characterized by four steps:

- Application of the antireflex paint L MR 2000 on the component (Fig. 1a)
- Application of the markers on a fixed base and constrain the component on it (Fig. 1b)
- 360-degree rotation of the scanner around the component (Fig. 1c)
- calibration of the markers on the model through proprietary software (Fig. 1d)

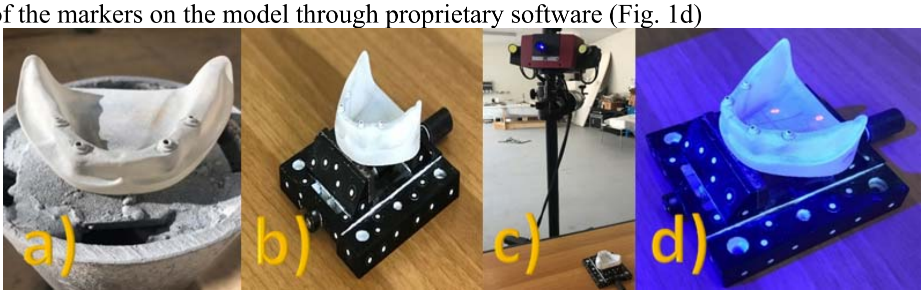

Fig. 1. a) L MR 2000 antireflex application on the model; b) Alignment of the model with the detection and application base of the markers c) Atos Compact Scan d) Calibration of the markers.

Once the markers had been calibrated, a standard polygon polygonization was carried out. Once obtained the model with the surfaces that approximate the assembly, Space Claim (software that uses rapid modelling tools to draw precise parts on mesh data) was used for geometry modelling. To create the implants and orient them in space, the axes that best approximated the position and orientation of the prosthesis were identified. Finally, the geometry was exported and the assembly cad was made.

2.3. FEM analysis

Once the 3d model was obtained, the authors focused on functionality, and on the type of connection between the components. For this reason, the dimensions of the cortical bone and the cancellous bone were schematized as in (Cervino et al., 2018; Cicciù et al., 2019, 2018). The bone was schematized as a cylindrical volume as in (Shelat et al., 2011). A number of 29 components were tested as described below in Fig. 2 (for each part of the assembly, markers were attributed). The identification numbers are as follow: abutment (1-4), screw (5-8), bridge (9), cortical bone (10-13), fixture (14-17), cancellous bone (18-21), seeger ring (22-25), equator (26-29).

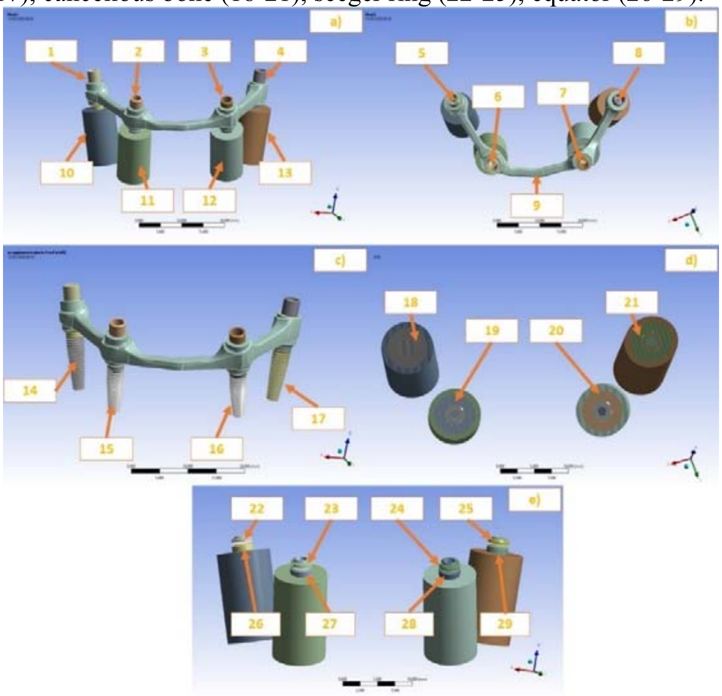

Fig. 2. a) Frontal view of assembly; b) top view of assembly; c) frontal view of prothesis; d) Section view of bone e) frontal view of Seegers.

2.4. System setup

Four different OT Bridge prosthesis system approaches for the rehabilitation of complete edentulism were analysed and compared. All systems used 4 implants and two of them (posterior prosthesis) are inclined as mentioned in Fig. 3b. A fixed connection with the prosthetic bar was modelled. The Seeger ring was connected inside the abutment (Fig. 3a), as specified by the manufacturer. The difference between the four-prosthesis system configuration consisted in the number of connection screws applied, respectively 4, 3, 2 and none.

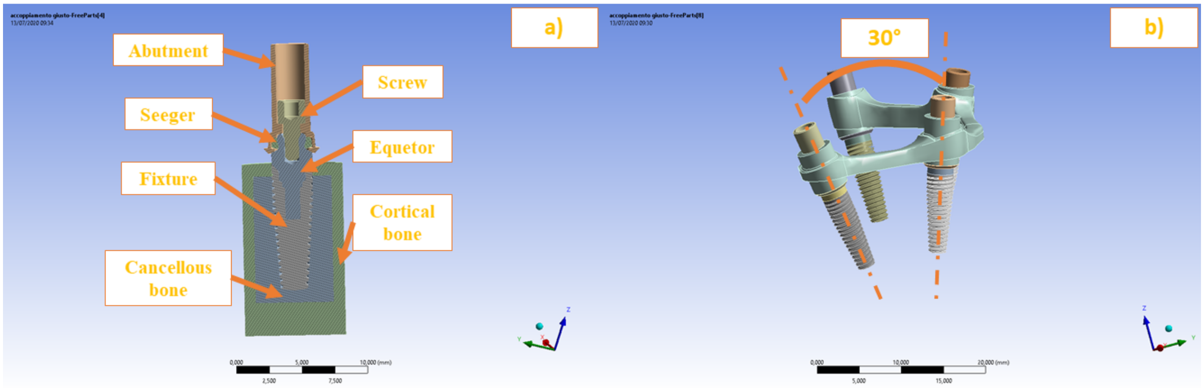

Fig. 3. a) Implant assembly scheme; b) Inclination angle of the posterior prostheses.

Table 1 show the mechanical characteristics used for the simulations. In particular, two different mechanical characteristics have been identified for the anterior and posterior areas for cortical and cancellous bone.

Table 1. Mechanical characteristics of all components.

Materials	Density [g/cm^3]	Young's modulus [N/mm^2]	Poisson's Ratio
Prosthesis	4.62	9.6E+04	0.360
Seeger	1.39	2.6E+03	0.350
Cortical Bone 4	1.8	1.93E+04	0.236
Cortical Bone 6	1.8	2.40E+04	0.236
Cancellous Bone 4	1.2	8.35E+02	0.236
Cancellous Bone 6	1.2	1.04E+03	0.236

2.5. Mesh and Boundary conditions

ANSYS Workbench was used to analyse all systems setup. In order to create a homogeneous and adequate mesh of the entire model, discretization tests revealed the difficulty of finding optimal solutions with a low number of elements. In particular, dimension of element was decreased in the zone of connection between Seeger and equator. Given the complexity of the geometry, second order tetragonal elements (SOLID186, average dimension 0.3 mm) were used to approximate it.

As reported in (Chrcanovic et al., 2016; Röhrle and Pullan, 2007; Toro-Ibacache et al., 2016), masticatory loads were applied on molars and constraints on bone. To evaluate the performance of this system, the perfect integration between prosthesis and bone were considered. The load was applied (on the negative z direction) on the abutments number 1 and 4, while the fixed constraints was applied on the cortical bone cylinders. As reported in (Cicciù et al., 2019), 0.3 friction coefficients were applied for the connection between the parts of the prosthesis. In particular, for the contact Seeger/Equator and Seeger/abutment, as reported in the catalogue of the producer, was defined a coefficient of friction of 0.35. Finally, the contact between the abutments and the bridge was considered as rigid.

3. Results and Discussion

3.1. Test 1

For the first test, the system with four screws connected was evaluated. Fig. 8a shows that the maximum values of Von Mises stress reached on the prosthesis are equivalent to 291 MPa, respectively on the contact area between part 14 and part 26, while for the surrounding bone the value found is equal to 83 MPa, on the contact area between part 14 and part 10. Furthermore, the posterior implants with prosthetic attachments are more stressed than the anterior ones. The simulated model is based on the scan of a real jaw; therefore, the implants are not mounted symmetrically. For this reason, the simulation (Fig. 4b) shows that the prosthesis are loaded, with greater intensity, on the left side (part 1-5-14-22-26). Stress analysis on the OT Equator/screw (Fig. 4c) interface shows the left rear attachment (part 5-26) is more stressed compared to the right rear attachment (part 8-29). Analysing in detail the four connection screws (Fig. 4d), the Von Mises stress distribution shows that the front left screw (part 6) is the most stressed since the load is more distributed on it, followed by the rear left one (part 5).

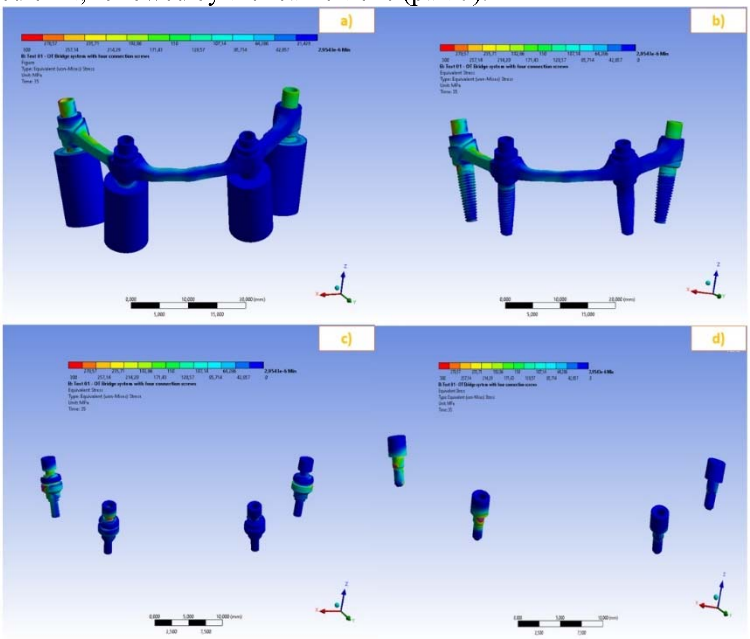

Fig. 4. a) Von Mises stress results for fixed prosthesis OT Bridge; b) Von Mises stress results for fixtures and prosthetic attachments; c) Von Mises stress results for interface OT Equator/connection screw; d) Von Mises stress related to the screws.

The focal point of this research is to evaluate the stability of the prosthesis. Total displacement and then the displacements along each single axis are calculated. The analysis shows that the displacements are greater at the prosthetic attachments (part 1) of the left posterior implant with a maximum peak of 0.2399 mm (Fig. 5a). Considering a single axis, the displacements along the X axis (Fig. 5b) are greater on the left (part 1) posterior abutment (0.22114 mm) while the maximum peak is 0.038072 mm for movements along the Y axis (Fig. 5c) in correspondence with the prosthetic attachments of the left posterior implant(part 1-26). Furthermore, there is a displacement along the positive y always in the same area and torsional moments along the X and Y axes. Finally, the displacements along the Z axis are analysed for the evaluation of a possible flexion of the prosthesis. Fig. 5d show that the displacement along the positive Z occurs on the prosthetic bar (part 9) between the two anterior abutments (part 2-3).

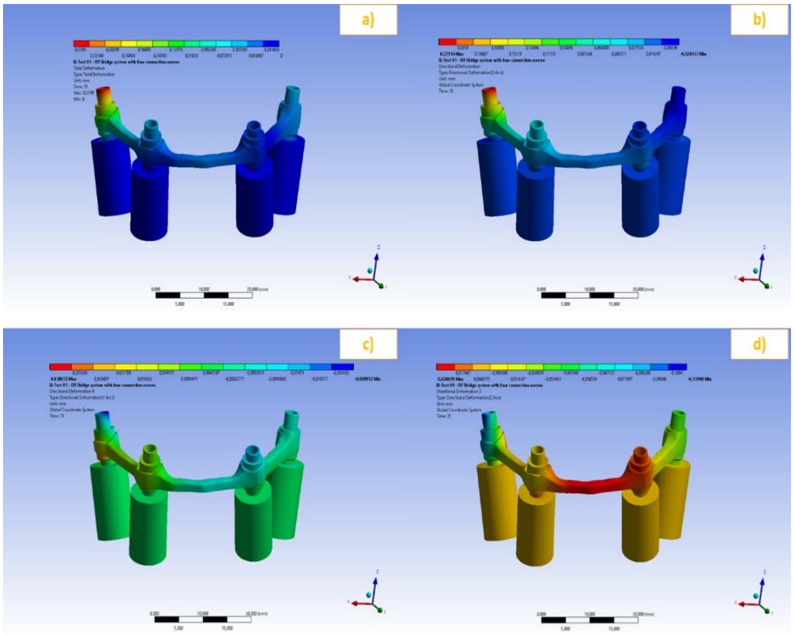

Fig. 5. a) Total displacement; b) Displacements along the X axis; c) Displacements along the Y axis; d) Displacements along the Z axis.

3.2. Test 2

For the second test, the system with three screws connected was evaluated. Fig. 6a show that the maximum values of Von Mises stress reached on the prosthesis are equivalent to 314 MPa, respectively on the contact area between part 14 and part 26 (Fig. 6c-e) while for the surrounding bone the value found is equal to 118 MPa, on the contact area between part 14 and part 10 (Fig. 6a-c). Furthermore, the posterior implants with prosthetic attachments are more stressed than the anterior ones. Fig. 6b shows that the prosthesis are loaded, with greater intensity, on the left side (part 1-5-14-22-26). Stress analysis on the OT Equator/screw (Fig. 6c) interface shows that there is more stressed in the left rear attachment (part 5-26) than the right rear attachment (part 8-29). Analysing in detail the four connection screws (Fig. 6d), the Von Mises distribution shows that the front left screw (part 6) is the most stressed since the load is more distributed on it, followed by the rear left one (part 5).

The analysis shows that the displacements are greater at the prosthetic attachments (part 1) of the left posterior implant with a maximum peak of 0.28569 mm (Fig. 7a). Considering a single axis, the displacements along the X axis (Fig. 7b) are greater on the left (part 1) posterior abutment (0.21641 mm) while the maximum peak is -0.1608 mm for movements along the Y axis (Fig. 7c) in correspondence with the prosthetic attachments of the left posterior implant(part 1-26). Furthermore, there is a displacement along the positive y always in the same area and torsional moments along the X and Y axes. Finally, the displacements along the Z axis are analysed for the evaluation of a possible flexion of the prosthesis. Fig. 7d show that the displacement along the positive Z occurs on the prosthetic bar (part 9) between the two anterior abutments (part 2-3).

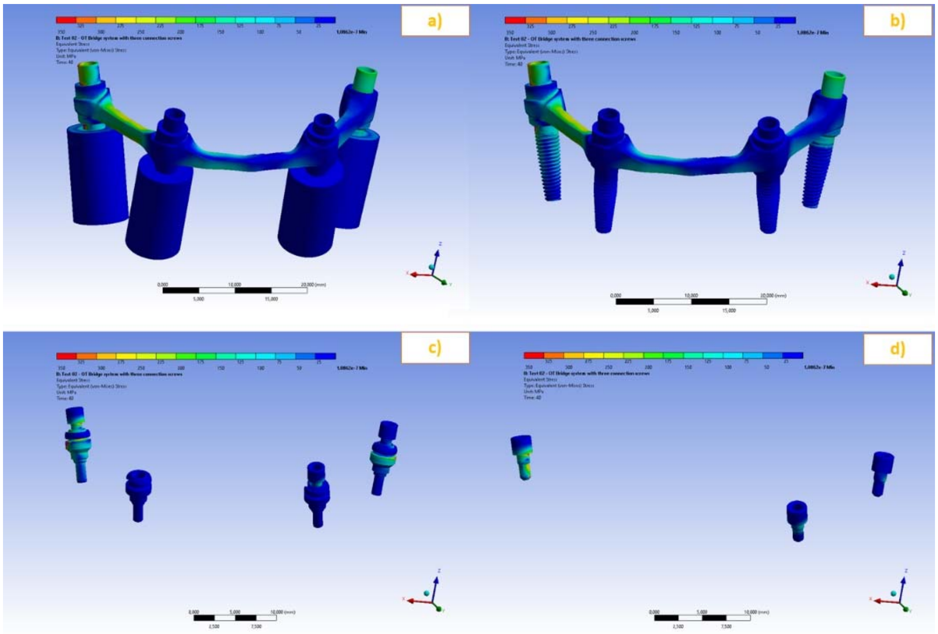

Fig. 6. a) Von Mises stress results for fixed prosthesis OT Bridge; b) Von Mises stress results for fixtures and prosthetic attachments; c) Von Mises stress results for interface OT Equator/connection screw; d) Von Mises stress related to the screws.

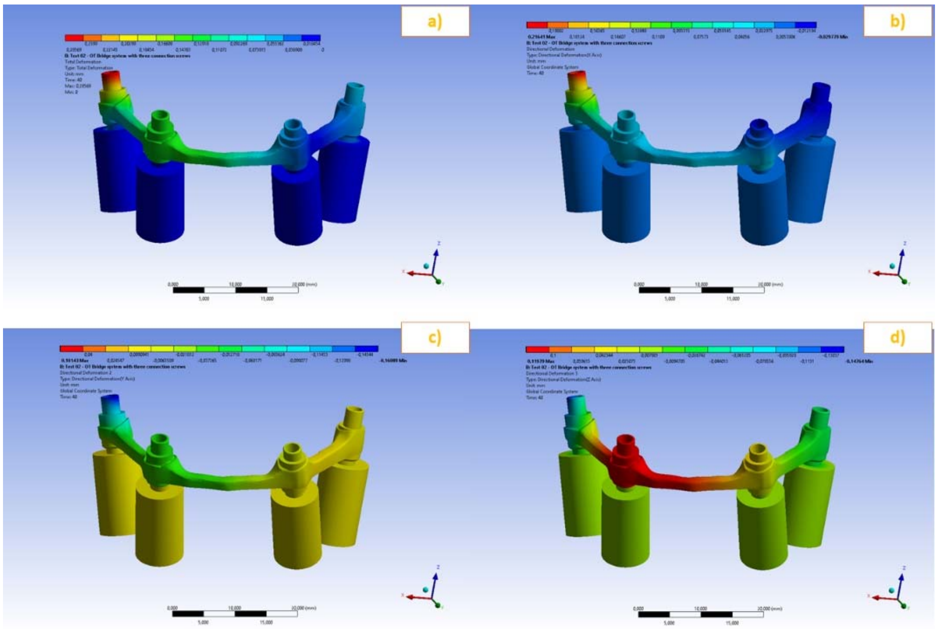

Fig. 7. a) Total displacement; b) Displacements along the X axis; c) Displacements along the Y axis; d) Displacements along the Z axis.

3.3. Test 3

For the third test was evaluated the system with two screws connected. Fig. 8a show that the maximum values of Von Mises stress reached on the prosthesis are equivalent to 346 MPa, respectively on the contact area between part 14 and part 26 while for the surrounding bone the value found is equal to 153 MPa, on the contact area between part

14 and part 10. Furthermore, the posterior implants with prosthetic attachments are more stressed than the anterior ones. Fig. 8b shows that the prosthesis are loaded, with greater intensity, on the left side (part 1-5-14-22-26). Stress analysis on the OT Equator-screw (Fig. 8c) interface shows that there is more stressed in the left rear attachment (part 5-26) than the right rear attachment (part 8-29). Analysing in detail the four connection screws (Fig. 8d), the Von Mises distribution shows that the front left screw (part 5) is the most stressed.

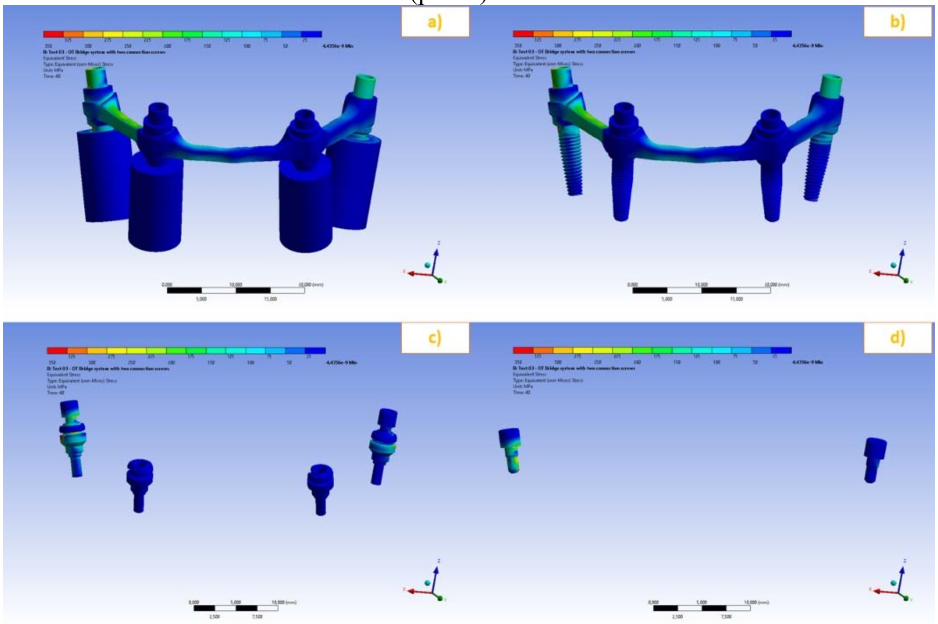

Fig. 8. a) Von Mises stress results for fixed prosthesis OT Bridge; b) Von Mises stress results for fixtures and prosthetic attachments; c) Von Mises stress results for interface OT Equator/connection screw; d) Von Mises stress related to the screws.

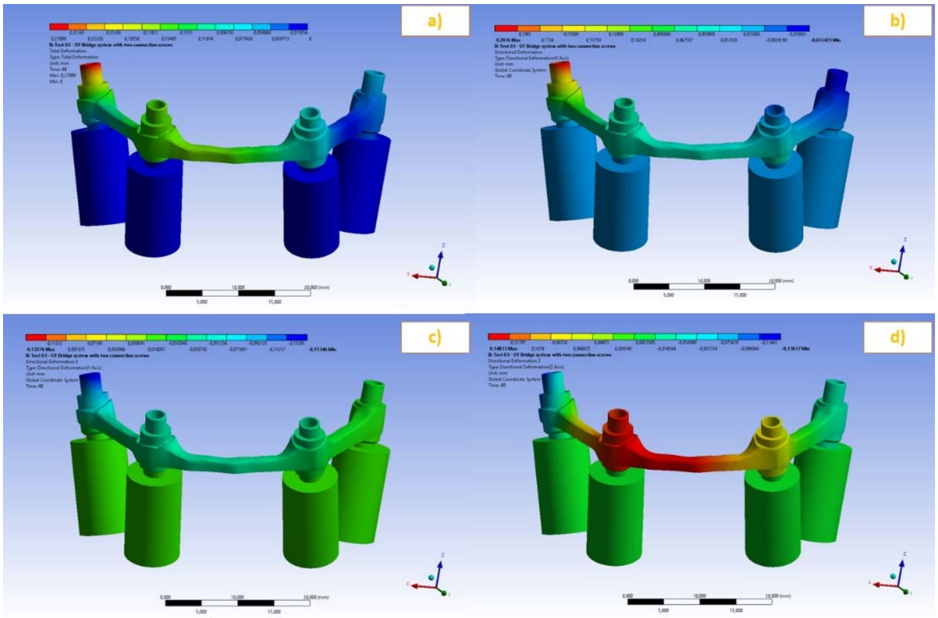

Fig. 9. a) Total displacement; b) Displacements along the X axis; c) Displacements along the Y axis; d) Displacements along the Z axis.

Total displacement and then the displacements along each single axis are calculated. The analysis shows that the displacements are greater at the prosthetic attachments (part 1) of the left posterior implant with a maximum peak of 0.29569 mm (Fig. 9a). Considering a single axis, the displacements along the X axis (Fig. 9b) are greater on the left (part 1) posterior abutment (0.2276 mm) while the maximum peak is -0.1708 mm for movements along the Y axis (Fig. 9c) in correspondence with the prosthetic attachments of the left posterior implant (part 1-26). Furthermore, there is a displacement along the positive y always in the same area and torsional moments along the X and Y axes. Finally, the displacements along the Z axis are analysed for the evaluation of a possible flexion of the prosthesis. Fig. 9d show that the displacement along the positive Z occurs on the prosthetic bar (part 9) between the two anterior abutments (part 2-3).

3.4. Test 4

For the fourth test, the system without screws connected was evaluated. Fig. 10a show that the maximum values of Von Mises stress reached on the prosthesis are equivalent to 208 MPa, respectively on the contact area between part 14 and part 26 (Fig. 10c-e) while for the surrounding bone the value found is equal to 83 MPa, on the contact area between part 14 and part 10 (Fig. 10a-c). Furthermore, the posterior implants with prosthetic attachments are more stressed than the anterior ones. Fig. 10b shows that the prosthesis are loaded, with greater intensity, on the left side (part 1-14-22-26). Stress analysis on the OT Equator (Fig. 10c) interface shows that there is more stressed in the left rear attachment (part 14-26) than the right rear attachment (part 17-29).

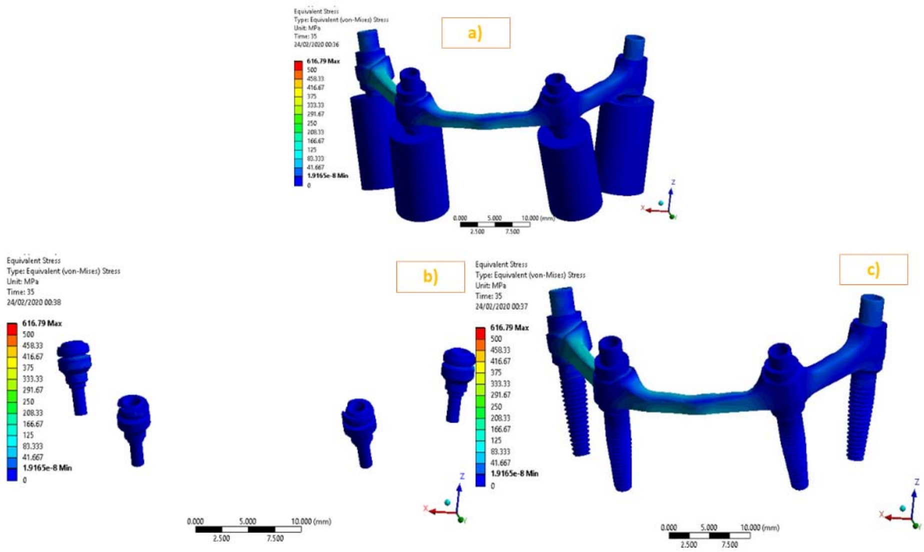

Fig. 10. a) Von Mises stress results for fixed prosthesis OT Bridge; b) Von Mises stress results for fixtures and prosthetic attachments; c) Von Mises stress results for interface OT Equator/connection screw; d) Von Mises stress related to the screws.

Total displacement and then the displacements along each single axis are calculated. The analysis shows that the displacements are greater at the prosthetic attachments (part 1) of the left posterior implant with a maximum peak of 0.37515 mm (Fig. 11a). Considering a single axis, the displacements along the X axis (Fig. 11b) are greater on the left (part 1) posterior abutment (0.15485 mm) while the maximum peak is -0.300 mm for movements along the Y axis (Fig. 11c) in correspondence with the prosthetic attachments of the left posterior implant(part 1-26). Furthermore, there is a displacement along the positive y always in the same area and torsional moments along the X and Y axes. Finally, the displacements along the Z axis are analysed for the evaluation of a possible flexion of the prosthesis. Fig. 11d show that the displacement along the positive Z occurs on the prosthetic bar (part 9) between the two anterior abutments (part 2-3).

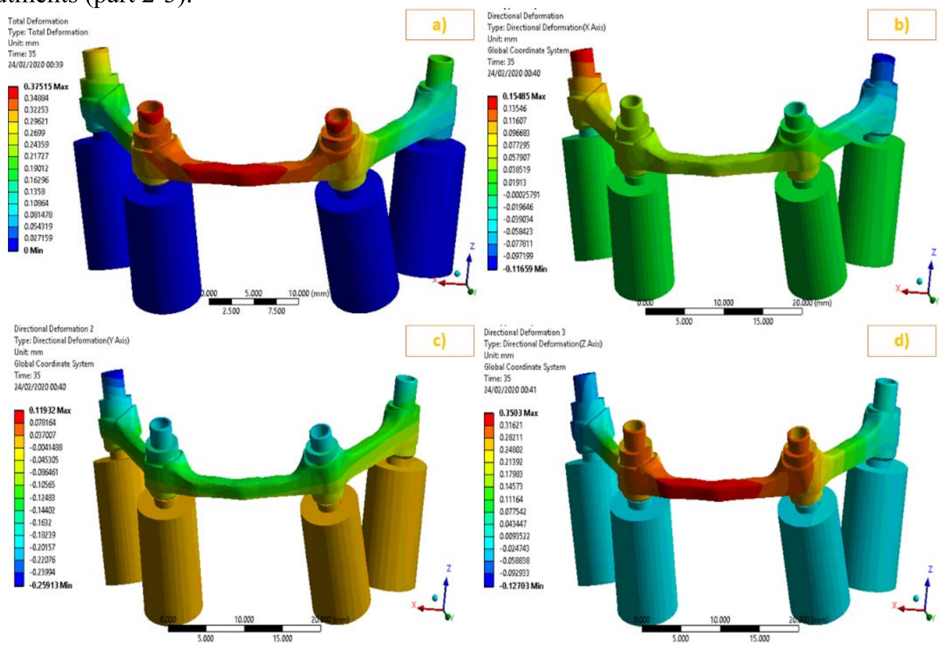

Fig. 11. a) Total displacement; b) Displacements along the X axis; c) Displacements along the Y axis; d) Displacements along the Z axis.

3.5. Summary

As described previously, the constraints applied on the system are the same for all four tests. The displacement along z axis major than height of Seeger was applied as a stopping criterion of the simulation. For this reason, for Test 3 and Test 4, respectively 700 N and 100 N, were applied on the molars, since for these loads the previously described condition is verified. Table 2 shows the maximum Von Mises stress calculated on the main stressed components of all tests.

Table 2. Max Von Mises (in MPa) stress for each test.

Part number	Test 1	Test 2	Test 3	Test 4
5 (screw)	267.06	203.81	318.32	-
6 (screw)	280.39	-	-	-
7 (screw)	101.22	202.37	-	-
8 (screw)	208.28	76.71	130.45	-
9 (bridge)	196.02	255.1	220.89	91.24
26 (equator)	291	314	346	2086

Analysing Table 2, it can be noticed that the most stressed component is part 26 (equator) (Test 1, 291 MPa; Test 2, 314 MPa; Test 3, 346 MPa; Test 4, 208 MPa). Test 3 returns the highest value of Von Mises for this component. By removing two connection screws (part 6-7), increases the stress on the same parts (part 5-8) and decreases on the bridge (part 9).

Table 3. Average Von Mises stress for each test.

Part number	Test 1	Test 2	Test 3	Test 4
1 (abutment)	152.83	162.79	178.895	70.2
6 (screw)	152.65	-	-	-
7 (screw)	50.81	102.39	-	-
10 (cortical bone)	44.275	64.52	81.11	44.42
11 (cortical bone)	20	20.76	0.195	0.665
12 (cortical bone)	3.265	3.755	0.067	3.098
13 (cortical bone)	42.715	44.46	66.45	56.145

Table 3 shows the average Von Mises stress calculated on the components of all tests. By removing two connection screws (part 6-7), increases the distribution of stresses on bone (part 10-13) and the highest stress distribution is localized on part 1 (left posterior abutment).

Table 4. Axial deformation for each test

Part number	Test 1			Test 2			Test 3			Test 4		
	x	y	z	x	y	z	x	y	z	x	y	z
1 (abutment)	0.221	-0.028	-0.12	0.23	-0.16	-0.14	0.24	-0.15	-0.12	0.15	-0.26	-0.12
2 (abutment)	0.066	0.045	0.01	0.022	-0.068	0.11	0.05	-0.07	0.12	0.0386	-0.24	0.314
3 (abutment)	-0.001	-0.014	0.03	-0.012	-0.006	0.04	0.01	-0.05	0.08	-0.039	-0.22	0.294
4 (abutment)	-0.0067	-0.08	-0.04	-0.029	0.009	-0.04	-0.03	-0.014	-0.01	-0.11	-0.14	0.35
9 (bridge)	0.13	0.03	0.02	0.12	-0.083	0.119	0.12	0.012	0.148	0.019	-0.16	-0.09

Finally, analysing Table 4 it can be noticed that decreasing the number of screws increases the motion of the implant, for this reason a twisting moment is generated on the bridge (Part 9). Test 3 is characterized by an increase in the torque on the bridge, located in the area of contact with part 2. Test 4, on the other hand, is characterized by a high displacement along the axis z which generates a rotation of the bridge which can cause the release of the prosthesis.

4. Conclusion

Scientific and clinical research has always invested in finding simple, repeatable and reliable protocols in order to facilitate the work of the dentist and dental technician. The implant-supported fixed prosthesis completely changes the physical and social condition of the edentulous patient. The OT Bridge system represents an original solution compared to fixed prostheses on the market thanks to its various prosthetic components that make it unique and versatile. The Seeger system could allow the elimination of many holes for the connection screws, especially in the aesthetic area, thanks to the retentive force of the acetal ring. In this regard, it is important to define a correct assembly criterion for the OT Bridge prosthesis in terms of stability. The first two configurations (Test 1 and Test 2), respectively with four and three connection screws, are safe since the stresses generated are lower than the yield points of the material and the prosthesis is stable. Test 3, in which only two connecting screws are used, highlights the possible instability of the system. In this case, although the load is 87% compared to the loads applied in the previous tests, the stresses that arise are 1.5 times higher than the first two tests. Finally, Test 4 highlights the possible instability of the prosthesis due to the failure to anchor with connection screws. Therefore, the recommended number of abutments without screws should be limited to one ensuring adequate stability of the OT Bridge prosthesis.

References

Cavallaro, J., Greenstein, G., 2011. Angled implant abutments: A practical application of available knowledge. ournal Am. Dent. Assoc. 142, 150–158. https://doi.org/10.14219/jada.archive.2011.0057

Cervino, G., Romeo, U., Lauritano, F., Bramanti, E., Fiorillo, L., D'Amico, C., Milone, D., Laino, L., Campolongo, F., Rapisarda, S., Cicciù, M., 2018. Fem and Von Mises Analysis of OSSTEM ® Dental Implant Structural Components: Evaluation of Different Direction Dynamic Loads. Open Dent. J. 12, 219–229. https://doi.org/10.2174/1874210601812010219

Cervino, Montanari, Santonocito, Nicita, Baldari, De Angelis, Storni, Fiorillo, 2019. Comparison of Two Low-Profile Prosthetic Retention System Interfaces: Preliminary Data of an In Vitro Study. Prosthesis. https://doi.org/10.3390/prosthesis1010007

Chatterjee, A., Ragher, M., Patil, S., Chatterjee, D., Dandekeri, S., Prabhu, V., 2015. Prosthetic management of malpositioned implant using custom cast abutment. J. Pharm. Bioallied Sci. https://doi.org/10.4103/0975-7406.163528

Chen, Z., Lin, C.Y., Li, J., Wang, H.L., Yu, H., 2019. Influence of abutment height on peri-implant marginal bone loss: A systematic review and meta-analysis. J. Prosthet. Dent. https://doi.org/10.1016/j.prosdent.2018.10.003

Cicciù, M., Cervino, G., Milone, D., Risitano, G., 2019. FEM analysis of dental implant-abutment interface overdenture components and parametric evaluation of Equator® and Locator® prosthodontics attachments. Materials (Basel). 12. https://doi.org/10.3390/ma12040592

Cicciù, M., Cervino, G., Milone, D., Risitano, G., 2018. FEM Investigation of the Stress Distribution over Mandibular Bone Due to Screwed Overdenture Positioned on Dental Implants. Materials (Basel). 11, 1512. https://doi.org/10.3390/ma11091512

Gandhi, P.V., Kalsekar, B.G., Patil, A.A., Kandi, N.S., 2019. A low-profile universal attachment system with housing welded to metal reinforcement framework to retain mandibular implant overdenture: A clinical report. J. Indian Prosthodont. Soc. https://doi.org/10.4103/jips.jips_129_19

Huang, Y., Wang, J., 2019. Mechanism of and factors associated with the loosening of the implant abutment screw: A review. J. Esthet. Restor. Dent. https://doi.org/10.1111/jerd.12494

Kao, H., Gung, Y., Chung, T., Hsu, M., 2008. The influence of abutment angulation on micromotion level for immediately loaded dental implants: a 3-D finite element analysis. Int. J. Oral Maxillofac. Implant. 23, 623–630.

Kiatkroekkrai, P., Takolpuckdee, C., Subbalekha, K., Mattheos, N., Pimkhaokham, A., 2020. Accuracy of implant position when placed using static computer-assisted implant surgical guides manufactured with two different optical scanning techniques: a randomized clinical trial. Int. J. Oral Maxillofac. Surg. https://doi.org/10.1016/j.ijom.2019.08.019

Lin, C., Wang, J., Ramp, L., Liu, P., 2008. Biomechanical Response of Implant Systems Placed in the Maxillary Posterior Region Under Various Conditions of Angulation, Bone Density, and Loading. Int. J. Oral Maxillofac. Implant. 23, 57–64.

Moeller, M., Duff, R., Razzoog, M., 2011. Rehabilitation of malpositioned implants with a CAD/CAM milled implant overdenture: a clinical report. J. Prosthet. Dent. 105, 143–146. https://doi.org/https://doi.org/10.1016/S0022-3913(11)00025-4

Omori, Y., Lang, N.P., Botticelli, D., Papageorgiou, S.N., Baba, S., 2020. Biological and mechanical complications of angulated abutments connected to fixed dental prostheses: A systematic review with meta-analysis. J. Oral Rehabil. https://doi.org/10.1111/joor.12877

Romeo, E., Chiapasco, M., Ghisolfi, M., Vogel, G., 2002. Long-term clinical effectiveness of oral implants in the treatment of partial edentulism: Seven-year life table analysis of a prospective study with ITI® Dental Implants System used for single-tooth restorations. Clin. Oral Implants Res. 13, 133–143. https://doi.org/10.1034/j.1600-0501.2002.130203.x

Roos-Jansåker, A.M., Lindahl, C., Renvert, H., Renvert, S., 2006. Nine- to fourteen-year follow-up of implant treatment. Part I: Implant loss and associations to various factors. J. Clin. Periodontol. 33, 283–289. https://doi.org/10.1111/j.1600-051X.2006.00907.x

Sannino, G., Barlattani, A., 2016. Straight Versus Angulated Abutments on Tilted Implants in Immediate Fixed Rehabilitation of the Edentulous Mandible: A 3-Year Retrospective Comparative Study. Int. J. Prosthodont. https://doi.org/10.11607/ijp.4448

Santonocito, D., Nicita, F., Risitano, G., 2021. A Parametric Study on a Dental Implant Geometry Influence on Bone Remodelling through a Numerical Algorithm. Prosthesis 3, 157–172. https://doi.org/10.3390/prosthesis3020016

Scrascia, R., Fiorillo, L., Gaita, V., Secondo, L., Nicita, F., Cervino, G., 2020. Implant-Supported Prosthesis for Edentulous Patient Rehabilitation. From Temporary Prosthesis to Definitive with a New Protocol: A Single Case Report. Prosthesis. https://doi.org/10.3390/prosthesis2010002

Scrascia, R., Martinolli, M., Venezia, P., Casucci, A., Ortensi, L., Tallarico, M., 2018. Feasibility of Low Profile Attachments to Improve Quality of Life on Patients with Implant-Retained Mandibular Overdenture: 1-Year Preliminary Results of a Multicenter Prospective Case Series Study. J. Oral Heal. Dent. Manag. 17, 5.

Shelat, S., Kularashmi, B., Annapoorani, H., Chakravarthy, R., 2011. Effect of two different abutment types on stress distribution in the bone around an implant under two loading conditions. J. Dent. Implant. https://doi.org/10.4103/0974-6781.91284

Tallarico, M., Caneva, M., Meloni, S.M., Xhanari, E., Covani, U., Canullo, L., 2018. Definitive Abutments Placed at Implant Insertion and Never Removed: Is It an Effective Approach? A Systematic Review and Meta-Analysis of Randomized Controlled Trials. J. Oral Maxillofac. Surg. https://doi.org/10.1016/j.joms.2017.08.025

Tallarico, M., Martinolli, M., Kim, Y.-J., Cocchi, F., Meloni, S.M., Alushi, A., Xhanari, E., 2019. Accuracy of Computer-Assisted Template-Based Implant Placement Using Two Different Surgical Templates Designed with or without Metallic Sleeves: A Randomized Controlled Trial. Dent. J. 7, 41. https://doi.org/10.3390/dj7020041

Tallarico, M., Meloni, S., Canullo, L., Xhanari, E., Polizzi, G., 2016. Guided surgery for single-implant placement: A critical review. J. Oral Sci. Rehabil. 2, 8–14.

Tallarico, M., Scrascia, R., Annucci, M., Meloni, S.M., Lumbau, A.I., Koshovari, A., Xhanari, E., Martinolli, M., 2020. Errors in Implant Positioning Due to Lack of Planning: A Clinical Case Report of New Prosthetic Materials and Solutions. Materials (Basel). 13, 1883.

https://doi.org/10.3390/ma13081883
Zitzmann, N.U., Margolin, M.D., Filippi, A., Weiger, R., Krastl, G., 2008. Patient assessment and diagnosis in implant treatment. Aust. Dent. J. https://doi.org/10.1111/j.1834-7819.2008.00036.x